Wind-Tunnel Wall Interference Effects for 20° Cone-Cylinders

JOHN WILLIAM DAVIS*
NASA Marshall Space Flight Center, Huntsville, Ala.

AND

ROBERT F. GRAHAM†
Northrop Services Inc., Huntsville, Ala.

Pressure data from 20° cone-cylinder models tested in a blowdown wind tunnel for the Mach number range 0.2 to 5.0 are compared to an interference-free standard to determine wall interference effects as a function of test section blockage. Four models representing a range of blockage from approximately 1% to 6% were compared to curve fits of the interference-free standard at each Mach number, and errors were determined at each pressure tap location. The average of the absolute values of the percent error over the length of the model based on an interference-free standard was determined and used as the criterion for evaluating model blockage interference effects. The results are presented in the form of the percent error as a function of model blockage and Mach number.

Nomenclature

A_0 = regression equation intercept coefficient
B_P = regression equation coefficient of Pth degree independent variable term
i = $1, 2, \ldots, n$
M = Mach number
n = number of model pressure measuring stations
P_L/P_T = ratio of local model static pressure to freestream total pressure
P_∞/P_T = ratio of freestream static pressure to freestream total pressure
X/D = model body station per unit diameter
$|\varepsilon|_{AVG}$ = average absolute percent error
$\bar{\varepsilon}_{AVG}$ = average arithmetic percent error

I. Introduction

HISTORICALLY, in discussions of wall corrections to wind-tunnel data there have been two approaches to the problem: 1) theoretical calculation of the interference effects and subsequent correction of the data, or 2) empirical development of walls which show as little interference as possible. In adopting the latter approach, the variable porosity wind tunnel has proven to be an excellent facility to minimize wall interference effects.[1] At the Marshall Space Flight Center's (MSFC) 14-in. Trisonic Wind Tunnel (TWT) excellent comparison with interference free data has been shown for a cone-cylinder model tested in the variable porosity transonic test section at approximately 1% blockage throughout the Mach range.[2] The need for testing models that have considerably more than 1% blockage has arisen in the past few years.

Therefore, the general problem becomes one of determining model size limitations and/or data correction techniques necessary for valid interference-free simulation. This formidable task involves model shape and size, model angle to the flow and location with respect to the tunnel wall, model support system, and additional flow parameters such as Mach number, Reynolds number, and stagnation pressure. To provide some guidelines for future tests, this study isolates two of these parameters, Mach number and model size, for a 20° cone-cylinder configuration. Tests were conducted in both the transonic and supersonic test sections of the MSFC TWT at Mach numbers from 0.2 to 5.0. The tunnel wall porosity and wall angle settings used at each test Mach number in the transonic test section were those optimum values[1] for a model of 0.901% blockage. After establishing an interference-free standard for each Mach range, the test program and equipment are described and the results presented. The final results are presented in average absolute percent error as a function of Mach number for models of varying degrees of test section blockage.

Presented as Paper 72-1010 at the AIAA 7th Aerodynamic Testing Conference, Palo Alto, Calif., September 13–15, 1972; submitted September 22, 1972, revision received May 14, 1973.

Index category: Aircraft Testing (Including Component Wind Tunnel Testing).

* Chief, Gas Dynamics Section. Associate Fellow AIAA.
† Senior Engineer. Member AIAA.

II. Interference-Free Standard

The experimental data from any wind tunnel contain some degree of interference from the walls and model support system that is not present under flight conditions. In an effort to evaluate the extent of this interference in the MSFC TWT, the 20° cone cylinder data from this tunnel are compared to an interference-free standard. The selection of this interference-free standard is subject to two variables: the flow regime, i.e., subsonic, transonic or supersonic; and the use of an analytical or experimental technique. The subsonic speed regime has been arbitrarily defined as the Mach range 0.2 to 0.6. The reference data in the transonic speed regime range from Mach 0.6 to 1.15 and in the supersonic speed regime range from Mach 1.15 to 5.0. Since the viscous effects are negligible from a 20° cone-cylinder at zero angle of attack, the powerful numerical techniques developed over the past two decades were chosen as the interference-free standard for both the subsonic and supersonic flow conditions. Due to the mathematical complexities involved in analytic techiques, the transonic interference-free standard is based on experimental data taken in much larger wind tunnels. Using these guidelines, the following discussion contains a general description of the various flow regime interference-free standards.

With the advent of the large scale computer, the method of linear integral equations has been used to solve the fundamental subsonic potential flow equations. One example of this type of solution is given by Smith and Pierce,[3] from which a computer analysis commonly referred to as the Douglas Neumann Program has been developed. The subsonic interference-free results involved in this report are calculated from an axisymmetric, compressible flow version of this program.

To establish an experimental interference-free standard for transonic flow, the data of Table 1 present some of the

Table 1 20° cone-cylinder data

Ref. no.	Investigator	Facility	Tunnel	Mach range	Model diameter cm	Model diameter in.	Percent blockage
8	Erickson & Dowling	Convair	HST 4 ft × 4 ft	0.8 → 1.1	8.839	3.480	0.412
11	Capone & Coates	Langley	16 ft Transonic	0.7 → 1.3	21.589	8.5	0.198
					15.240	6.0	0.098
					3.810	1.5	0.0062
9	Mitchell	Lewis	8 ft × 6 ft Supersonic	0.5 → 2.0	40.640	16	2.91
					30.480	12	1.64
					20.320	8	0.73
					10.160	4	0.18
5	Robertson & Chevalier	AEDC	1 ft Transonic	0.5 → 1.2	2.540	1	0.5
					3.810	1.5	1.23
4	Estabrooks	AEDC	1 ft Transonic	0.7 → 1.4	2.540	1	0.5
					4.864	1.915	2.0
					6.878	2.708	4.0
			16 ft Transonic	0.7 → 1.4	54.864	21.6	1.0
					4.864	1.915	0.008
6	Anderson, Anderson & Credle	AEDC	1 ft Transonic	0.6 → 1.3	3.439	1.354	0.945
10	Hartley & Jacocks	AEDC	16 ft Transonic	0.6 → 1.6	13.757	5.416	0.0625
7	Jacocks	AEDC	4 ft Transonic	0.6 → 1.2	13.757	5.416	1.0

investigations that were studied. Previous studies with transonic interference-free data have almost universally used the data from Estabrooks[4] that were taken in the Arnold Engineering Development Center (AEDC) 16-ft transonic tunnel (16T). These data were not available in tabulated form and were therefore very difficult to treat in this report due to the use of the computer in the analysis of the data. The more recent data from the AEDC 1-ft and 4-ft transonic tunnels[5–7] and the Convair High Speed tunnel[8] were rejectcd as interference-free standards because of a relatively high percent blockage. The data from the NASA Lewis 8- by 6-ft tunnel[9] could not be used because of the extensive disturbances caused by the nonporous sections of the tunnel. Although it exhibited some interference effects near Mach 1.0, the Hartley and Jacocks data from the AEDC 16T[10] were chosen as the interference-free standard for this study and were used in the plotted comparisons shown in Figs. 3–5 (discussed later). After this selection, the data of Capone and Coates from the Langley 16-ft transonic tunnel[11] became available and were used as the interference-free standard for the final error analysis portion of this study. These data show negligible wave interference. Additional data may be found in Refs. 12–18.

In the supersonic flow regime the well-known method of characteristics has been used to determine the interference-free standard. The method of characteristics analysis used to compute the results presented in this report was developed by Sims[19] for axisymmetric flow and has been refined over the past decade.

III. Experimental Procedure

The purpose of this test program was to provide a preliminary guide to blockage effects in a variable porosity wind tunnel throughout the complete Mach range. The following discussion describes the characteristics of the wind tunnel, the models, and the test procedure.

The 14-in. Trisonic Wind Tunnel

The MSFC TWT is a blowdown wind tunnel employing interchangeable test sections each 14 in. (35.56 cm) square and 20 in. (50.80 cm) in length. The variable porosity transonic test section is used at Mach numbers from 0.2 to 1.96. The range of porosities used is between 0.5% and 5.4% with the holes slanted 60° upstream. A single optimum (based on 0.901% blockage, 20° cone-cylinder test results) wall porosity and wall angle combination is employed at each test Mach number in the transonic test section[1] as shown in Table 2. Testing at Mach numbers from 2.74 to 5.00 is accomplished in the solid wall supersonic test section.

The tunnel run time is approximately 80 sec and the Reynolds number ranges from 1 to 18 million per foot (0.3 to 5.4 million per meter). A description of the variable porosity walls and their optimum configuration as a function of Mach number is given by Felix,[1] and a complete description of the tunnel and its operating parameters is given by Simon in a technical handbook.[20]

The 20° Cone-Cylinder Models

The model and support configurations used in this report are given in Table 3, and Fig. 1 illustrates the model dimensions and their test locations in the MSFC TWT. Configurations

Table 3 Model and support configurations

Model diameter in.	Model diameter cm	Model blockage %	Sting diameter (see Ref. 20) in.	Sting diameter (see Ref. 20) cm	Sting extension (see Ref. 20)
1.915	4.864	1.469	0.875	2.223	52
2.710	6.883	2.943	0.875	2.223	53
3.318	8.428	4.412	0.875	2.223	53
3.833	9.736	5.887	0.875	2.223	53

Table 2 Transonic test section wall configuration

Mach number	0.2 to 0.95	1.00	1.05	1.10	1.15	1.20	1.30	1.46	1.96
Wall porosity, %	5.4	0.5	0.75	1.6	5.4	5.4	5.4	5.4	5.4
Wall angle, min	D[a] 15	[b]C 15	C 15	C 15	D 15	0	D 15	0	0

[a] D indicates diverged walls.
[b] C indicates converged walls.

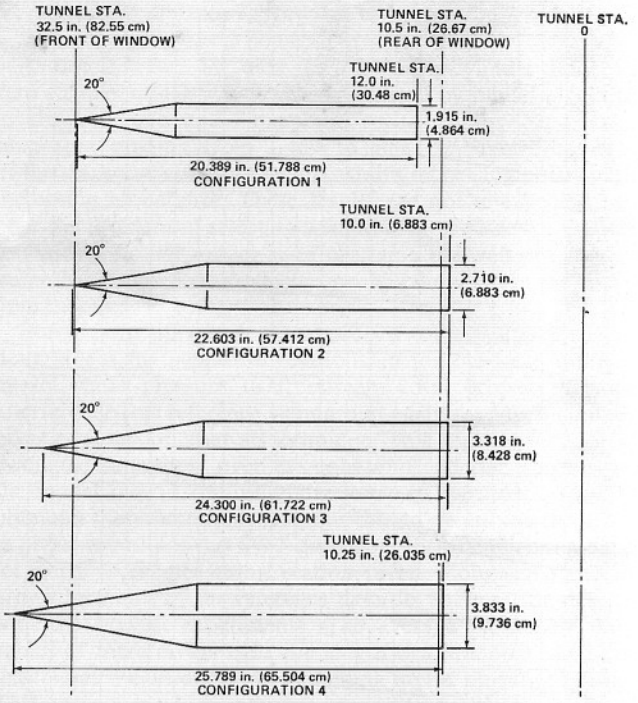

Fig. 1 Model dimensions and test locations for the five configurations.

1 and 2 were tested by Estabrooks[4] and are noted in Table 1. These configurations have a series of nose shapes in addition to the sharp apex cone (no bluntness) that is the subject of this report.

Test Procedure

The test program investigated four model configurations ranging in percent blockage from 1.469 to 5.887 through the Mach range 0.2 to 5.0. For Mach 0.2 to 1.96, the stagnation pressure was 137,000 N/m² (20 psia) using the transonic variable porosity test section. Stagnation pressures for the supersonic solid wall tests were 345,000 N/m² (50 psia) at Mach 2.74, 3.0 and 3.5, and 689,500 N/m² (100 psia) at Mach 4.0, 4.5, and 5.0.

IV. Experimental Results for the 20° Cone-Cylinders

The experimental results are presented in the form of pressure distributions at a given Mach number for all four models in Figs. 2–6. These figures graphically demonstrate the effect of model blockage.

Figure 2 compares pressure data with Douglas-Neumann analysis[3] presented as a function of body station X/D for various size models at $M = 0.4$ and is representative of the low subsonic results. The agreement is excellent. In general, the effect of model blockage at this Mach number is small with the flow acceleration at the base of the larger models not simulated by the Douglas-Neumann analysis.

The TWT pressure data shown in Fig. 3 for Mach number 0.95 is plotted for comparison with the Douglas-Neumann analysis and the AEDC 16T data.[10] This figure shows an appreciable difference between the three plotted results. The Douglas-Neumann is not capable of simulating the terminal shock which begins to appear on the conical portion of the model just above Mach 0.8 and has progressed to just aft of the cone-cylinder junction at Mach 0.9. Ericsson[17] gives a good picture of the development of this terminal shock. Neglecting the Douglas-Neumann data, there is a pronounced effect of model blockage. The increase in model blockage causes the pressure rise to move slightly upsteam. The pressure

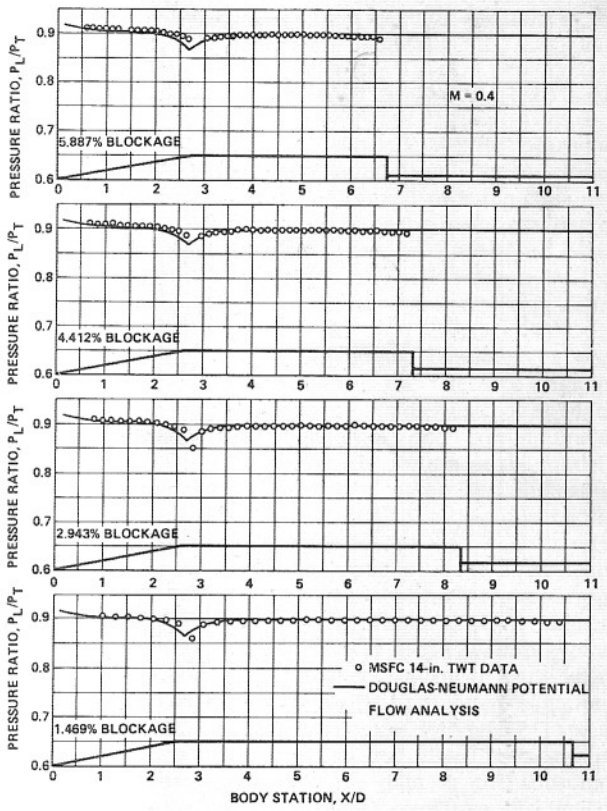

Fig. 2 Pressure distributions on a 20° cone-cylinder effect of model blockage, $M = 0.4$.

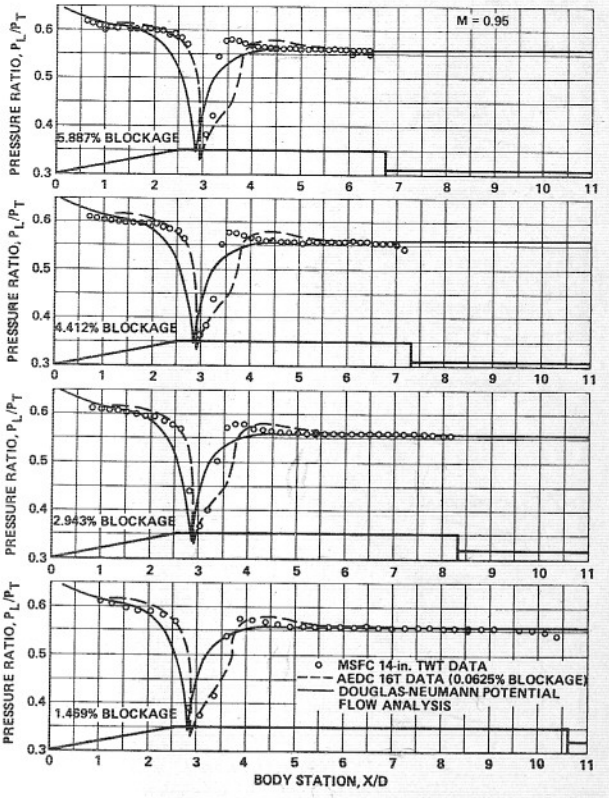

Fig. 3 Pressure distributions on a 20° cone-cylinder effect of model blockage, $M = 0.95$.

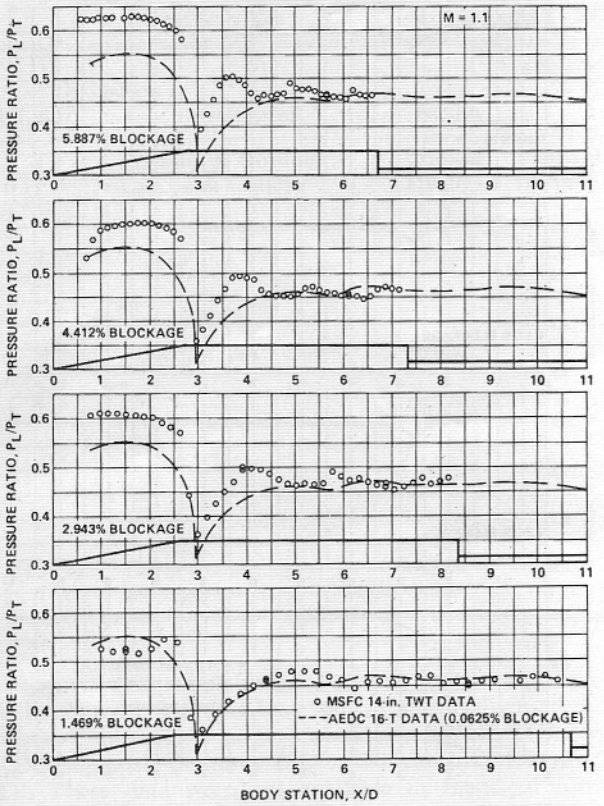

Fig. 4 Pressure distributions on a 20° cone-cylinder effect of model blockage, $M = 1.1$.

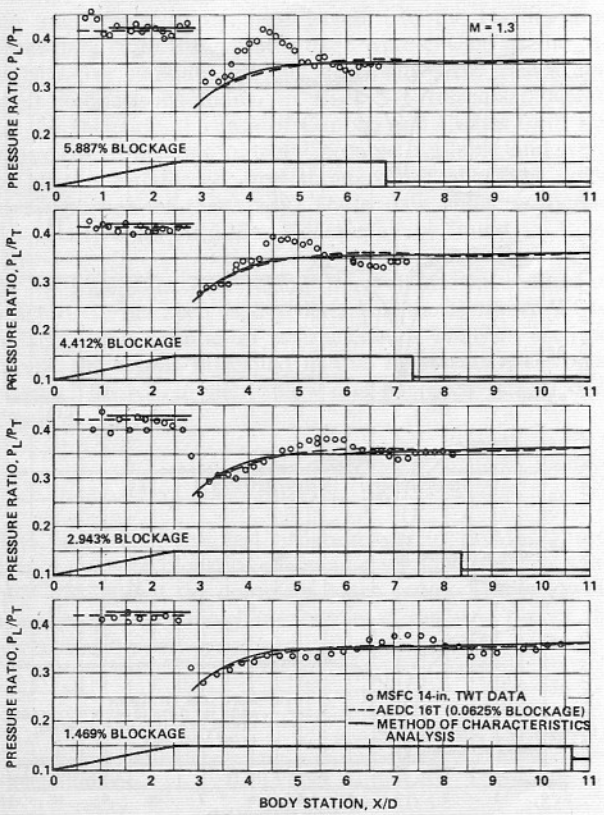

Fig. 5 Pressure distributions on a 20° cone-cylinder effect of model blockage, $M = 1.3$.

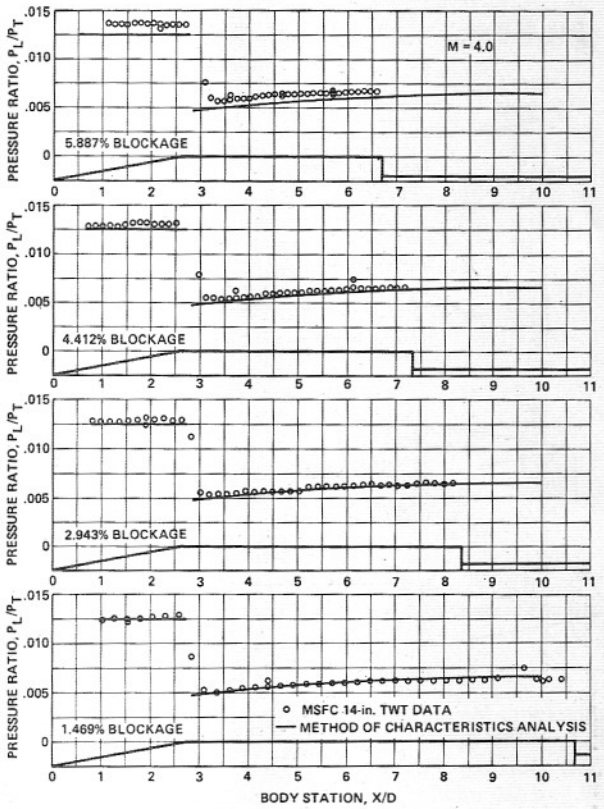

Fig. 6 Pressure distributions on a 20° cone-cylinder effect of model blockage, $M = 4.0$.

ratio increases, for the AEDC 16T data are not completely interference free at this Mach number, exhibiting a noticeable dip in the pressure after the cone-cylinder junction. Figure 4 presents the MSFC 14-in. TWT data for Mach number 1.1 plotted for comparison with the AEDC 16T data. In attempting to analyze these data, a statement quoted in a number of AEDC reports may be of some help. "If the wall is too open, the bow shockwave will be reflected as an expansion wave and the shoulder expansion fan will be reflected as a compression wave, and if the wall is too solid, the bow shockwave will reflect as a compression wave and the shoulder expansion fan will reflect as expansion waves."

The AEDC 16T data seem to exhibit a small compression wave at body station 6 (Fig. 4) which according to the above criteria could be interpreted as a reflected shoulder expansion fan for a wall that is too open or a bow shock reflection for a wall that is too solid. Hartley and Jacocks[10] note this interference but do not comment on the cause. The MSFC 14-in. TWT data show a definite effect of model blockage with the most disturbing aspect being the increase in the pressure ratio on the cone with increased blockage. This seems to indicate that (neglecting the possibility of impingement on the cone of an uncancelled bow wave) the local Mach number behind the bow wave changes as the model blockage increases. This phenomenon make the interpretation of downstream disturbances very difficult.

Pressure data shown in Fig. 5 for Mach number 1.3 are plotted for comparison with the AEDC 16T and the Method of Characteristics (MOC) analysis.[19] This figure shows an increase in compression reflection for the larger models. This seems to indicate that the bow shock is reflecting as a compression wave, leading to the conclusion that the walls are too solid for the higher blockages. This condition continues at higher Mach numbers until the reflection moves aft of the largest model at Mach 3.5 and does not reappear. Figure 6 presents pressure data for Mach 4.0 which show little effect of model blockage.

V. Analysis of Data Errors due to Increasing Model Size

As noted in Sec. IV, data for a 20° cone-cylinder model at zero angle of attack was largely unaffected by model blockage in the subsonic and supersonic speed ranges for model blockages ranging from 1.469 to 5.887%. However, data in the transonic speed range did exhibit increasing errors with increasing model size. These results are not unexpected but pose the problem of selecting a suitable model size for a given test with a similar model or of changing the wall porosity to minimize interference effects, or a combination of both approaches.

For present purposes, the approach to this problem is to determine a mathematical relationship for the local ratio of model static pressure to freestream total pressure for an interference-free reference standard at each test Mach number using a regression analysis technique. This analytic function is evaluated separately over the cone and cylinder portions of the model due to the different nature of the flow. Having obtained these functions, it is possible to determine the error in pressure ratio of the TWT data from the reference standard for each local measuring station, even though the model orifice locations of the reference data do not coincide exactly with the present experiments. The average of the absolute values of these errors over the length of the model has been selected as the criterion for evaluating model blockage effects. This procedure will be covered later in more detail.

Interference-Free Reference Data

Analytical predictions were made in the subsonic speed range by the Douglas-Neumann potential flow theory and by the method of characteristics in the supersonic speed range as discussed earlier. In the transonic speed range, experimental data obtained from a very small model tested in a large wind tunnel which could be assumed to be free of wall interference are available, and data in this range from the NASA Langley Research Center 16-ft tunnel[11] were selected for the baseline in analyzing data errors for the four different size models.

Using these various reference data as input, relations of the form

$$P_L/P_T = A_0 + B_1(X/D) + B_2(X/D)^2 + \cdots + B_P(X/D)^P \quad (1)$$

were determined at each test Mach number (as nearly as possible) by digital computation using a technique developed in Ref. 21. Separate fits were determined over the cone and over the cylinder portions of the model for various degree relationships and the best fits selected for further use based on an assessment of the maximum absolute percent error, the average absolute percent error, the correlation coefficient, and the F statistic.

In each case, fourth-order polynomial relationships were selected as the best representation of the reference data for the cone and cylinder at each Mach number (except at Mach number of 1.15 and greater where a horizontal straight line of given intercept was used for the cone portion of the model). The equations selected and statistical parameters indicating their significance are shown in Table 4 for the cone and in Table 5 for the cylinder portion of the model. The fits were well-behaved with excellent correlation with the interference free reference data. The fitted ranges applicable to the various reference relations are shown in Table 6. The highest average percent error for any fit was 1.256%, with typical values being around 0.5%. Other statistical parameters indicated that it is highly probable that the fitted equations do accurately represent the reference standard. Typical plots indicating the correlation of the fitted relationships with the reference interference-free data in the subsonic, transonic, and supersonic speed ranges are shown in Fig. 7.

Determination of Error of TWT Model Data with Respect to the Interference-Free Reference Standard

Having determined mathematical expressions for the interference-free reference standard, it is possible to determine the error at any nondimensional distance along the model for each test Mach number. The average of the absolute values

Table 4 Curve fit parameters for cone portion of reference data[a]

M	A_0	B_1	B_2	B_3	B_4	Maximum percent error	Average percent error	R
0.200	0.9767	0.1140×10^{-2}	-0.7438×10^{-2}	0.5626×10^{-2}	-0.1291×10^{-2}	0.053	0.028	0.995
0.300	0.9486	0.5050×10^{-2}	-0.2097×10^{-1}	0.1525×10^{-1}	-0.3414×10^{-2}	0.215	0.085	0.991
0.400	0.9120	0.4047×10^{-2}	-0.2766×10^{-1}	$0.2102 - 10^{-1}$	-0.4851×10^{-2}	0.219	0.113	0.995
0.500	0.8679	0.5765×10^{-2}	-0.4179×10^{-1}	0.3200×10^{-1}	-0.7411×10^{-2}	0.355	0.181	0.996
0.600	0.8180	0.1072×10^{-1}	-0.6148×10^{-1}	0.4623×10^{-1}	-0.1061×10^{-1}	0.549	0.272	0.996
0.703	−0.5059	0.3116×10^{-1}	-0.2800×10^{1}	0.1076×10^{1}	−0.1510	1.530	0.640	0.991
0.802	−0.7071	0.3477×10^{1}	-0.3130×10^{1}	0.1205×10^{1}	−0.1693	1.862	0.816	0.991
0.905	−0.7167	0.3349×10^{1}	-0.2988×10^{1}	0.1136×10^{1}	−0.1574	1.879	0.844	0.989
0.954	−0.8537	0.3608×10^{1}	-0.3194×10^{1}	0.1204×10^{1}	−0.1652	1.898	0.938	0.986
1.000	−0.9100	0.3715×10^{1}	-0.3282×10^{1}	0.1234×10^{1}	−0.1686	1.974	1.098	0.980
1.038	-0.1105×10^{1}	0.4118×10^{1}	-0.3611×10^{1}	0.1350×10^{1}	−0.1843	2.066	1.144	0.974
1.104	-0.1166×10^{1}	0.4155×10^{1}	-0.3635×10^{1}	0.1354×10^{1}	−0.1825	2.146	1.186	0.951
1.150[b]	0.5060	0.000	0.000	0.000	0.000	...	...	...
1.200[b]	0.4658	0.000	0.000	0.000	0.000	...	...	...
1.300[b]	0.4204	0.000	0.000	0.000	0.000	...	...	...
1.460[b]	0.3255	0.000	0.000	0.000	0.000	...	...	...
1.960[b]	0.1650	0.000	0.000	0.000	0.000	...	...	...
2.740[b]	0.5962×10^{-1}	0.000	0.000	0.000	0.000	...	...	...
3.000[b]	0.4222×10^{-1}	0.000	0.000	0.000	0.000	...	...	...
3.500[b]	0.2242×10^{-1}	0.000	0.000	0.000	0.000	...	...	...
4.000[b]	0.1244×10^{-1}	0.000	0.000	0.000	0.000	...	...	...
4.500[b]	0.7214×10^{-2}	0.000	0.000	0.000	0.000	...	...	...
5.000[b]	0.4362×10^{-2}	0.000	0.000	0.000	0.000	...	...	...

[a] Reference data: $M = 0.20$ to 0.60 Douglas-Neumann potential flow theory; $M = 0.703$ to 1.104 LRC 16-ft experimental data; $M = 1.15$ to 5.00 method of characteristics.

[b] B coefficients are zero since horizontal straight line of given intercept was used.

Table 5 Curve fit parameters for cylinder portion of reference data[a]

M	A_0	B_1	B_2	B_3	B_4	Maximum percent error	Average percent error	R
0.20	0.9520	0.9281×10^{-2}	-0.1444×10^{-2}	0.9219×10^{-4}	-0.2061×10^{-5}	0.235	0.054	0.882
0.30	0.8952	0.2013×10^{-1}	-0.3139×10^{-2}	0.2006×10^{-3}	-0.4490×10^{-5}	0.517	0.118	0.884
0.40	0.8196	0.3432×10^{-1}	-0.5324×10^{-2}	0.3389×10^{-3}	-0.7565×10^{-5}	1.026	0.220	0.873
0.50	0.7420	0.4336×10^{-1}	-0.6325×10^{-2}	0.3751×10^{-3}	-0.7738×10^{-5}	1.745	0.373	0.862
0.60	0.6052	0.8406×10^{-1}	-0.1369×10^{-1}	0.9194×10^{-3}	-0.2169×10^{-4}	2.521	0.550	0.869
0.703	0.3492	0.2191	-0.4778×10^{-1}	0.4510×10^{-2}	-0.1559×10^{-3}	0.748	0.198	0.964
0.802	0.1828	0.2820	-0.6202×10^{-1}	0.5891×10^{-2}	-0.2045×10^{-3}	0.845	0.235	0.972
0.905	-0.2136×10^{1}	0.1758×10^{1}	−0.4098	0.4098×10^{-1}	-0.1490×10^{-2}	1.503	0.266	0.832
0.954	-0.2162×10^{1}	0.1632×10^{1}	−0.3563	0.3363×10^{-1}	-0.1162×10^{-2}	4.064	1.256	0.986
1.000	−0.9991	0.8614	−0.1811	0.1669×10^{-1}	-0.5683×10^{-3}	1.342	0.522	0.997
1.038	−0.8912	0.7978	−0.1696	0.1578×10^{-1}	-0.5419×10^{-3}	1.208	0.538	0.996
1.104	−0.7173	0.6823	−0.1459	0.1362×10^{-1}	-0.4686×10^{-3}	1.085	0.446	0.996
1.150	−0.7522	0.6945	−0.1507	0.1430×10^{-1}	-0.4988×10^{-3}	1.569	0.546	0.998
1.200	−0.6117	0.5931	−0.1284	0.1218×10^{-1}	-0.4255×10^{-3}	1.582	0.485	0.998
1.300	−0.3998	0.4285	-0.9081×10^{-1}	0.8465×10^{-2}	-0.2912×10^{-3}	1.536	0.412	0.999
1.460	−0.2065	0.2600	-0.5379×10^{-1}	0.4933×10^{-2}	-0.1678×10^{-3}	1.023	0.300	0.999
1.960	-0.3280×10^{-1}	0.7715×10^{-1}	-0.1460×10^{-1}	0.1251×10^{-2}	-0.4043×10^{-4}	0.533	0.146	1.000
2.740	-0.2658×10^{-2}	0.1876×10^{-1}	-0.3369×10^{-2}	0.2810×10^{-3}	-0.8954×10^{-5}	0.275	0.074	1.000
3.000	-0.1027×10^{-3}	0.1139×10^{-1}	-0.1983×10^{-2}	0.1614×10^{-3}	-0.5043×10^{-5}	0.518	0.069	1.000
3.500	0.9220×10^{-3}	0.4772×10^{-2}	-0.7997×10^{-3}	0.6365×10^{-4}	-0.1961×10^{-5}	0.537	0.069	1.000
4.000	0.7731×10^{-3}	0.2173×10^{-2}	-0.3570×10^{-3}	0.2824×10^{-4}	-0.8709×10^{-6}	1.164	0.097	1.000
4.500	0.1424×10^{-2}	0.4592×10^{-3}	-0.2939×10^{-4}	-0.8916×10^{-6}	0.1125×10^{-6}	0.897	0.163	1.000
5.000	0.3737×10^{-2}	0.5225×10^{-3}	-0.8361×10^{-4}	0.6614×10^{-5}	-0.2062×10^{-6}	1.579	0.108	1.000

[a] Reference data: $M = 0.20$ to 0.60 Douglas-Neumann potential flow theory; $M = 0.70$ to 1.10 LRC 16-ft experimental data; $M = 1.15$ to 5.00 method of characteristics.

Table 6 Fitted ranges of reference data

Number	Cone	Cylinder
0.200 to 0.600	X/D from 0.100 to 2.700	X/D from 2.843 to 10.000
0.703 to 1.104	X/D from 1.063 to 2.813	X/D from 3.063 to 9.813
1.150 to 5.000	X/D from 0.000 to 2.836	X/D from 2.836 to 10.000

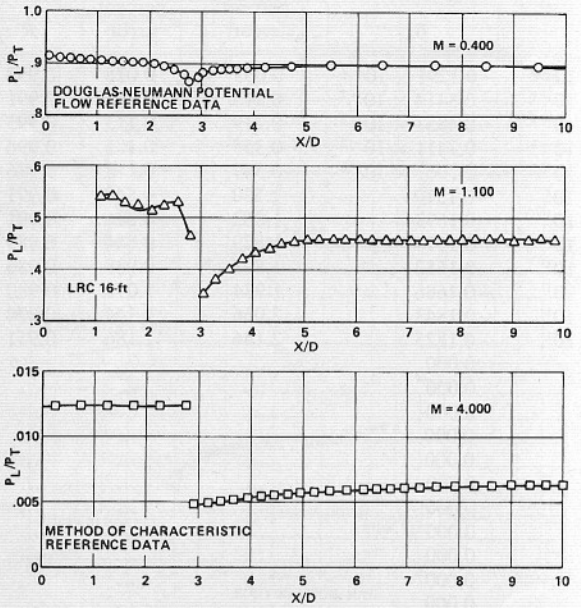

Fig. 7 Comparison of 20° cone-cylinder fitted equation results with interference-free reference data.

of the percent error over the length of the model is defined by

$$|\bar{\varepsilon}|_{AVG} = \frac{1}{n}\sum_{i=1}^{n}\left|\frac{(P_L/P_{T_{EXP}}) - (P_L/P_{T_{REF}})}{P_L/P_{T_{REF}}}\right| \times 100 \qquad (2)$$

where n is the number of model pressure measuring stations and $P_L/P_{T_{REF}}$ is determined from Eq. (1) at the given Mach number and X/D pressure measuring location. By this means, the average absolute error over the length of the model was obtained for each of the four different model sizes at each Mach number tested. The error was evaluated over the cone portion of the model for X/D values from 1.063 to 2.813 and over the cylinder portion of the model for X/D values from 3.063 to 9.813.

Results of this analysis are shown in Fig. 8 as a function of Mach number. Since the test Mach number range was 0.2 to 5.0, the ratio of freestream static pressure to stagnation pressure varied from approximately unity at the lowest Mach number to near zero at the highest Mach number. Therefore the data in Fig. 8 are normalized by multiplying the average absolute percent error by the ratio of freestream static pressure to the stagnation pressure to compare blockage effects on a roughly equivalent basis (in terms of experimental resolution).

In general, the data shown in Fig. 8 exhibit the expected trends. In the subsonic range, the error due to model blockage is negligible for the range of blockages tested. Data obtained in the supersonic test section ($M \geqq 2.74$) are fairly closely

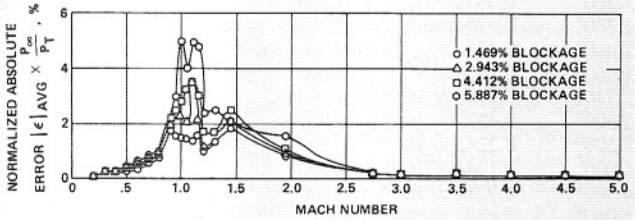

Fig. 8 Relationship of normalized absolute error to freestream Mach number for each model tested.

grouped for all models tested indicating little blockage effect, although at high supersonic Mach numbers the local pressure ratios approach zero and experimental resolution of the local model pressure ratios becomes difficult. As indicated in Fig. 8, the critical region for blockage effects occurs in the transonic speed range where increasing blockage clearly results in increasing average absolute percent error.

Within the transonic speed range the general trend, considering all model blockages as a group, indicates low errors at the lower Mach numbers, rises to a peak value at approximately Mach number 1.10, and then decreases to lower values until Mach number 1.20 is reached. At this Mach number, the optimized settings of the TWT variable porosity walls have reached the full open position of the walls (5.4% porosity) and no further increase in wall porosity is possible. Some reflected wave interference could be expected at higher transonic Mach numbers since optimization of the wall configuration is not possible. Results at AEDC indicate that at least 8% porosity is required to accommodate the full range of transonic testing at optimum wall conditions.[7] Thus the measured error over the 20° cone-cylinder model rises somewhat in the nonoptimized region above Mach 1.2 to a maximum value at Mach 1.46 and then decreases with increasing Mach number. It then appears that higher porosity walls are in order for the TWT in this unoptimized region and effects are underway to provide 10% variable porosity walls for the facility. Further, an inspection of Fig. 8 reveals that several relatively small slope reversals of the error curve occur at discrete Mach numbers within the range of sonic nozzle testing. This suggests the need for further refinement of the wall configuration to optimize wall cancellation.

It is recalled that the basic acceleration of the test gas in the transonic test section at Mach numbers 1.46 and 1.96 is provided by converging diverging nozzles with the porous walls serving to remove the test section boundary layer and cancel incident wave systems. Under these conditions, a discontinuity in the wall porosity curve as a function of Mach number might be expected when compared to lower Mach number testing with the sonic nozzle. The present standard wall settings at Mach numbers 1.46 and 1.96 use the maximum 5.4% porosity of the total wall. As shown in Fig. 9, an assessment of the arithmetic percent error (to be discussed later) shows that at Mach 1.46 the error is positive, again indicating that more porosity is required to cancel the incident shock wave. Similar results were also obtained at Mach 1.96. However, Fig. 9 shows at Mach numbers from 1.15 to 1.30 the error for the smallest model tested is negative, indicating a slightly overcorrected situation with perhaps too large a wall porosity being used. The larger models, however, show positive errors in this range.

It has been noted that the errors due to model blockage for typical force tests appear to be less than those obtained with pressure models. Evidently this is due to the probability that errors of different signs exist over different regions of the model, due primarily to the reflective properties of uncancelled shock and expansion waves in the critical transonic speed range, and that these errors tend to cancel when integrated over the length of the model. To assess this process, the average arithmetic percent error over the length of the model has been determined as follows:

$$\bar{\varepsilon}_{AVG} = \frac{1}{n}\sum_{i=1}^{i=n}\left(\frac{(P_L/P_{T_{EXP}}) - (P_L/P_{T_{REF}})}{P_L/P_{T_{REF}}}\right) \times 100 \qquad (3)$$

A comparison of the average arithmetic percent error and the average of the absolute values of the percent error over the length of the cone-cylinder model as a function of Mach number is shown in Fig. 9 in the transonic speed range for each blockage value tested. Results indicate slightly lower arithmetic errors for the 2.943, 4.412, and 5.887% blockage models and drastically reduced errors for the 1.469% blockage model throughout the transonic speed range. Thus, the

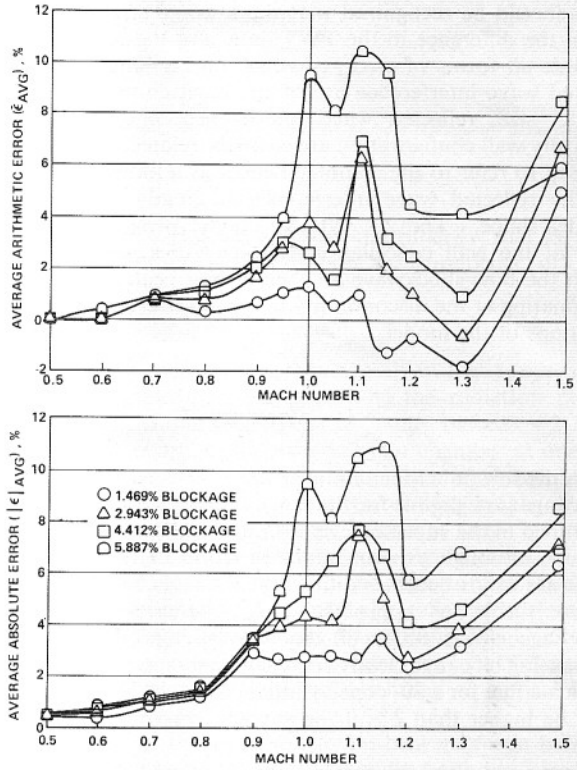

Fig. 9 Comparison of absolute and arithmetic errors in critical transonic speed range.

desirability of limiting model blockage to approximately 2% or less for similar models is indicated.

To assess the blockage parameter directly as a guide for designing future tests with similar models, a plot of the average absolute percent error for the 20° cone-cylinder model with respect to blockage for zero angle of attack is shown in Fig. 10 for various Mach numbers in the critical transonic speed range. This plot indicates that if one wishes to design an experiment for a similar type model with an average absolute error in pressure ratio over the model of 5% (a reasonable figure for pressure models), the model blockage should be no higher than 2% if the test is to encompass the entire Mach number range, or no higher than 3% if testing at Mach number 1.10 is eliminated (or higher errors accepted at this condition).

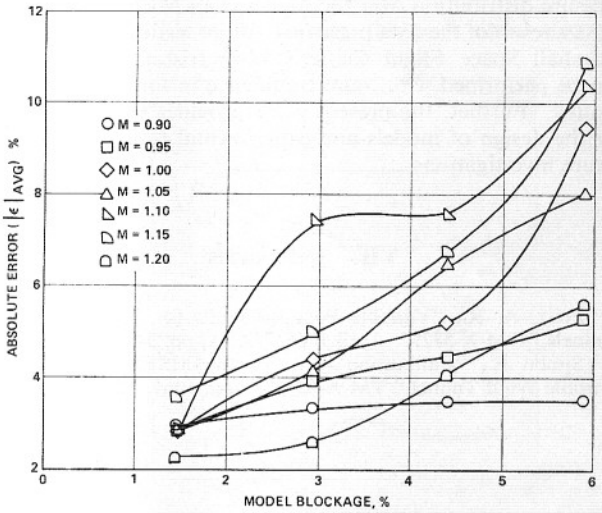

Fig. 10 Average absolute percent error in relation to model blockage in critical transonic speed range.

It should be recognized that the average errors computed from the difference in the TWT data and the reference data include all forms of error, of which model blockage and reflected wave interference are of the most concern. Since the model size, reflected wave interference, and the variable porosity wall configuration are strongly related,[21] it has been chosen to refer to the combined effect as a blockage effect.

The reflected wave interference is greatly dependent on model shape. The 20° cylinder model provides a difficult test of the wall cancellation characteristics with respect to both the bow shockwave and the strong centered expansion originating at the discontinuity between the cone and cylinder portions of the model.

VI. Summary

In the subsonic Mach number range, the error due to model blockage is negligible for the range of blockages tested. Data obtained in the supersonic speed range indicate little blockage effects, although experimental resolution of the local model pressure ratios becomes difficult at the higher Mach numbers where the ratios approach zero. The critical region for blockage effects occurs in the transonic speed range where increasing blockage clearly results in increasing error. Results indicate that for a 20° cone-cylinder the model blockage should not be higher than 2% if the average absolute error is to be limited to 5% or less.

Some unoptimized reflected wave interference should be expected during tests in the TWT transonic test section at Mach numbers greater than 1.2 due to wall porosity limitations. Higher porosity walls to be available in the future and additional wall optimization tests should correct this situation. The present standard optimum variable porosity wall configuration produces excellent results at Mach numbers of 1.2 and below, although some refinement is possible at discrete test Mach numbers. Testing in the transonic test section at Mach numbers of 1.3, 1.46, and 1.96 with full open walls provides adequate but not optimum wave cancellation.

Theoretical analysis by the Douglas-Neumann potential flow theory has provided interference-free reference pressure distributions for the 20° cone-cylinder model at subsonic Mach numbers, and analysis by the method of characteristics provides this information in the supersonic speed range. Experimental data obtained from a small model tested in the NASA Langley Research Center 16-ft tunnel have been used as the interference-free baseline in the transonic speed range. Mathematical relationship obtained by regression analysis from the reference data provide useful representations of the pressure distribution over the model from Mach 0.2 to 5.0.

As a result of the data presented, future testing in the NASA Marshall Space Flight Center's 14-in trisonic wind tunnel can be performed with more confidence in the quality of the results. Further, the present work provides useful guidance for the design of models and experimental test programs for future investigations.

VII. References

[1] Felix, A. R., "Variable Porosity Walls for Transonic Wind Tunnels," TM X-53295, April 1965, NASA, pp. 54–58.

[2] Simon E., "Calibration Tests of the MSFC 14- × 14-Inch Trisonic Wind Tunnel," TM X-53113, Aug. 1964, NASA.

[3] Smith, A. M. O. and Pierce, J., "Exact Solutions of the Neumann Problem. Calculation of Non-Circulatory Plane and Axially Symmetric Flows About or Within Arbitrary Boundaries," Rept. ES 26988, April 1958, Douglas Aircraft Co., Inc., Long Beach, Calif.

[4] Estabrooks, B. B., "Wall Interference Effects on Axisymmetric Bodies in Transonic Wind Tunnels with Perforated Wall Test Sections," AEDC-TR-59-12, June 1958, Arnold Engineering Development Center, Tullahoma, Tenn.

[5] Robertson, J. E. and Chevalier, H. L. "Characteristics of Steady-State Pressures on the Cylindrical Portion of Cone-Cylinder Bodies at Transonic Speeds," AEDC-TDR-63-104, Aug. 1963, Arnold Engineering Development Center, Tullahoma, Tenn.

[6] Anderson, C. F., Anderson, A., and Credle, O. P., "The Effect of Plenum Volume on the Test Section Flow Characteristics of a Perforated Wall Transonic Wind Tunnel," AEDC-TR-70-220, Oct. 1970, Arnold Engineering Development Center, Tullahoma, Tenn.

[7] Jacocks, J. L., "Determination of Optimum Operating Parameters for the AEDC-PWT-4-Foot Transonic Tunnel with Variable Porosity Test Section Walls," AEDC-TR-69-164, Aug. 1969, Arnold Engineering Development Center, Tullahoma, Tenn.

[8] Erickson, E. W. and Dowling, E. D., "Transonic Pressure Tests on a Series of 3.480 Inch Diameter Cone-Cylinder Models in the Convair High Speed Wind Tunnel," HST-TR-021-0, April 1961, Convair Aerospace/General Dynamics, San Diego, Calif.; see also Bates, D. R., "Cone-Cylinder Afterbody Normal Force Mach = 0.60 to 1.41," GD-BTD64-108, June 1964, Convair Div. of General Dynamics, San Diego, Calif.

[9] Mitchell, G. A., "Blockage Effects of Cone-Cylinder Bodies on Perforated Wind Tunnel Wall Interference," TM X-1655, Oct. 1968, NASA.

[10] Hartley, M. S. and Jacocks, J. L., "Static Pressure Distributions on Various Bodies of Revolution at Mach Numbers from 0.60 to 1.60," AEDC-TR-68-37, March 1968, Arnold Engineering Development Center, Tullahoma, Tenn.

[11] Capone, F. J. and Coates, E. M., "Determination of Boundary-Reflected-Disturbance Lengths in the Langley 16-Foot Transonic Tunnel," TN D-4153, Sept. 1967, NASA.

[12] Hauser, R. J., "Experimental Pressure and Normal Force Distribution Data for a Family of Cone-Cylinder Configurations at Test Mach Numbers from 0.7 to 2.0," LMSC/HREC-A710143, March 1965, Lockheed Missiles & Space Co., Huntsville, Ala.

[13] Page, W. A., "Experimental Study of the Equivalence of Transonic Flow About Slender Cone-Cylinder of Circular and Elliptic Cross Section," TN 4233, April 1958, NACA.

[14] Coe, C. F. and Kashley, A. J., "The Effects of Nose Bluntness on the Pressure Fluctuations Measured on 15 and 20 Degree Cone-Cylinders at Transonic Speeds," TM X-779, Jan. 1963, NASA.

[15] Jacocks, J. L., "Reduction of Wall Interference Effects in the AEDC-PWT 1-Foot Transonic Tunnel with Variable Perforated Walls," AEDC-TR-69-86, April 1969, Arnold Engineering Development Center, Tullahoma, Tenn.

[16] Jackson, F. M., "Calibration of the AEDC-PWT 1-Foot Transonic Tunnel with Variable Porosity Test Section Walls," AEDC-TR-69-114, May 1969, Arnold Engineering Development Center, Tullahoma, Tenn.

[17] Ericsson, L. E., "Steady and Unsteady Terminal-Shock Aerodynamics on Cone-Cylinder Bodies," LMSC/HREC L-87-67-2, Oct. 1967, Lockheed Missiles & Space Co., Huntsville, Ala.

[18] Yoshihara, H., "On the Flow Over a Cone-Cylinder Body at Mach Number One," TR 52-295, Nov. 1952, Wright Air Development Center, Dayton, Ohio.

[19] Sims, J. L., "Zero Angle-of-Attack Method of Characteristics," *Programmers User Manual*, MSFC Job 371440, Jan. 31, 1970, NASA.

[20] Simon, E., "The George C. Marshall Space Flight Center's 14 × 14-Inch Trisonic Wind Tunnel Technical Handbook," TM X-64624, Nov. 1971, NASA.

[21] Davis, J. W., "An Empirical Technique for Optimization of Variable Porosity Transonic Wind Tunnel Flows," Ph.D. dissertation, July 1972, Oklahoma State Univ., Stillwater, Okla.

Journal of Spacecraft and Rockets

VOLUME 10 NUMBER 10 OCTOBER 1973

SYNOPTICS

CONTRIBUTED PAPERS

ENGINEERING NOTES

ERRATA

A Publication of the American Institute of Aeronautics and Astronautics Devoted to Astronautical Science and Technology

JSCRAG 10 (10) 625–688 (1973)